



OPEN

Synergistic strengthening of polyelectrolyte complex membranes by functionalized carbon nanotubes and metal ions

SUBJECT AREAS:

POLYMERS

ORGANIC-INORGANIC
NANOSTRUCTURESReceived
16 September 2014Accepted
15 December 2014Published
14 January 2015Correspondence and
requests for materials
should be addressed to
Q.-F.A. (anqf@zju.
edu.cn)Tao Liu¹, Quan-Fu An¹, Qiang Zhao¹, Jia-Kai Wu¹, Yi-Hu Song¹, Bao-Ku Zhu¹ & Cong-Jie Gao^{2,3}

¹MOE Key Laboratory of Macromolecule Synthesis and Functionalization, Department of Polymer Science and Engineering, Zhejiang University, Hangzhou 310027, China, ²Department of Chemical Engineering and Bioengineering, Zhejiang University, Hangzhou 310027, China, ³The Development Center of Water Treatment Technology, Hangzhou 310012, China.

Hydrophilic polymers have garnered much attention due to their critical roles in various applications such as molecular separation membranes, bio-interfaces, and surface engineering. However, a long-standing problem is that their mechanical properties usually deteriorate at high relative humidity (RH). Through the simultaneous incorporation of functionalized carbon nanotubes and copper ions (Cu²⁺), this study introduces a facile method to fabricate high strength polyelectrolyte complex nanohybrid membranes resistant to high RH (90%). For example, the tensile strength of the nanohybrid membranes is 55 MPa at 90% RH (80% of the original value at 30% RH). These results are explained by copper ions depressing the swelling degree of the membrane, and functionalized carbon nanotubes promoting stress transfer between the polymer matrix and them. The nanohybrid membranes are efficient in separating water/alcohol mixtures containing relatively high water content (up to 30 wt%), whereas common hydrophilic polymer membranes usually suffer from excessive swelling under this condition.

Hydrophilic polymers, such as poly (vinyl alcohol), polyethylene glycol, polyelectrolytes, hydrogels, and so on, have attracted tremendous attention due to their high hydrophilicity, flexibility, and biocompatibility^{1–3}. They have been widely used in membrane separation, surface/interface engineering, controlled release, and tissue engineering^{4–7}. Hydrophilic polymers naturally absorb water and swell when exposed to a humid atmosphere, which negatively affects their mechanical properties and thus restricts their practical applicability. For example, proton exchange membrane fuel cells are commonly operated at an atmosphere of 90% relative humidity (RH) in order to achieve high conductivity. However, operating at high RH induces excessive swelling, causing mechanical failures that hamper the durability of these membranes⁸. Ikkala et al reported that the tensile strength of poly (vinyl alcohol) nanocomposites was 170 MPa at 25% RH, but this value decreased to 70 MPa at 85% RH⁹. Starch-based films, which are used as packaging material due to their low permeability to gases, also suffer from the decreased performance at high RH¹⁰. As such, there is a need for moisture resistant, high strength, polymer materials.

Chemical crosslinking can effectively guard the stability of hydrophilic polymers against humidity¹¹. However, chemical crosslinking also changes hydrophilicity of a material, limiting its the practical applications. Recently it was shown that doping hydrophilic polymers with multivalent metal ions is a versatile protocol to improve their mechanical strength at high RH^{12,13}. Unfortunately, the effect of this strategy on non-mechanical properties has been largely unexplored.

Polyelectrolyte complexes (PECs) are formed when two oppositely charged polyelectrolytes interact with each other in solution or at an interface¹⁴. PECs have been formed as colloidal dispersions, layer-by-layer assembled membranes, and porous bulk materials in various applications^{15–17}. PECs are commonly hydrophilic, giving them the potential to be applied as functional membranes for molecular separation, as gas barriers, and for energy conversion^{18–21}. However, absorption of water by hydrophilic PECs results in the rapid decay of mechanical strength²² and, more importantly, negatively affects the relevant properties for their applications^{23,24}. In this regard, although metal ion doping has been reported to enhance mechanical properties of polyelectrolyte mem-



branes^{25,26}, less is known regarding the effect this has on the functional membrane performance in high RH environments common in practical applications^{27,28}.

Recently, we developed a novel method to prepare PEC nanohybrid membranes displaying high mechanical strength, good barrier properties, and excellent molecular separation^{29–31}. However, both the mechanical properties and the separation performance declined rapidly at high RH due to excessive swelling. In order to solve this problem, we employed poly (sodium 4-styrenesulfonate) (PSS) functionalized carbon nanotubes (CNT-PSS) and copper ions to synergistically enhance the strength of PEC membranes in an atmosphere of high RH. First, the introduction of CNT-PSS facilitates load transfer from the polymer matrix to the nanofillers, which improves the tensile strength at low RH. Meanwhile, the chelate structure formed after doping the membrane with copper ions may serve to impede the absorption of water and reduce the plasticizing effects of water at high RH. Owing to the synergistic combination of CNT-PSS and copper ions, the prepared membranes exhibit good tensile strength at high RH, giving values of 55 MPa at 90% RH and 43 MPa in a 30 wt% water/isopropanol mixture. More importantly, we tested the molecular separation performance of the membrane using a high water content feed. We found that the water content of the permeate was improved from 90 wt% to 96 wt% as exemplified by the pervaporation dehydration of aqueous isopropanol containing 30 wt% water. A model mechanism is proposed to rationalize the performance in terms of a synergistic enhancement by CNT-PSS and copper ions.

Results and Discussion

Fabrication of PEC nanocomposites. The PEC nanocomposites (PEC/CNT-PSS) were fabricated *in situ* by incorporation of CNT-PSS into PEC³¹. Typically, an aqueous dispersion of CNT-PSS (0.4 g L⁻¹) was obtained by ultrasonication treatment (40 kHz, 100 W) for 1 h. Subsequently, 25 mL of the CNT-PSS dispersion solution was mixed with poly (2-methacryloyloxy ethyl trimethylammonium chloride) (PDMC) to obtain a 0.01 M solution (100 mL). The as-prepared polycation solution (PDMC@CNT-PSS) was added dropwise into 0.01 M carboxymethyl cellulose (CMC) solution (200 mL) (Step 1, Fig. 1). Both of the PDMC@CNT-PSS and CMC solutions contained the same concentration of HCl (0.009 M).

Finally, the precipitates were collected when the CMC was fully neutralized. The precipitates were dried at 60°C for 12 h (Step 2, Fig. 1). 0.2 g PEC/CNT-PSS was dissolved in 10 mL 0.1 M NaOH to obtain a 2 wt% homogenous dispersion. The free-standing PEC/CNT-PSS membrane was obtained by casting this solution onto a clean glass slide and drying at 40°C for 12 h (Step 3, Fig. 1). Copper ion doped PEC (PEC/Cu) membranes and copper ion doped PEC/CNT-PSS (PEC/CNT-PSS/Cu) membranes were obtained after infiltration of copper ions into PEC and PEC/CNT-PSS membranes, respectively. The infiltration of copper ions was achieved by soaking the membrane in a 3 wt% CuCl₂ solution (Step 4, Fig. 1). Afterward the membranes were removed from the 3 wt% CuCl₂ solution, they were washed with a 10 wt% water/isopropanol mixture and dried at 30°C for 12 h (Step 5, Fig. 1).

Characterizations of CNT-PSS and PEC/CNT-PSS membranes.

The acid-treated CNTs, CNT-PSS, and PSS were characterized by FTIR (Fig. 2a). The characteristic absorption of CNT-PSS at 1040 cm⁻¹ is assigned to the SO₃⁻ groups, suggesting that PSS was successfully grafted onto CNTs³². Both the acid-treated CNTs and CNT-PSS exhibit a carbonyl peak at 1730 cm⁻¹ attributed to -COOH groups resulting from the oxidation treatment. TGA curves show that 18 wt% PSS is grafted onto the CNT surface (Fig. S2).

Moreover, TEM characterization (Fig. S3) shows a rough layer on the outside of the modified nanotubes, indicating that PSS chains were grafted onto the outer surface of the nanotubes³³. As such, CNT-PSS can be uniformly dispersed in PEC matrix, mostly as single nanotubes without noticeable agglomeration (Fig. 2b). The thermal behavior of PEC and PEC/CNT-PSS membranes was investigated (Fig. S4). The residual weight of PEC/CNT-PSS containing 2 wt% content of CNT-PSS was observed to be approximately 1.8 wt% greater than pristine PEC membranes, indicating of the successful introduction of CNT-PSS.

Synergistic enhancement of tensile strength with resistance to high RH.

With the successful incorporation of CNT-PSS, we set out to study the effect of CNT-PSS content on mechanical properties of the PEC/CNT-PSS membranes. Notably, after loading a very small amount of CNT-PSS (1.0 wt%), the tensile strength (82 MPa) and elongation at break (4.8%) were readily

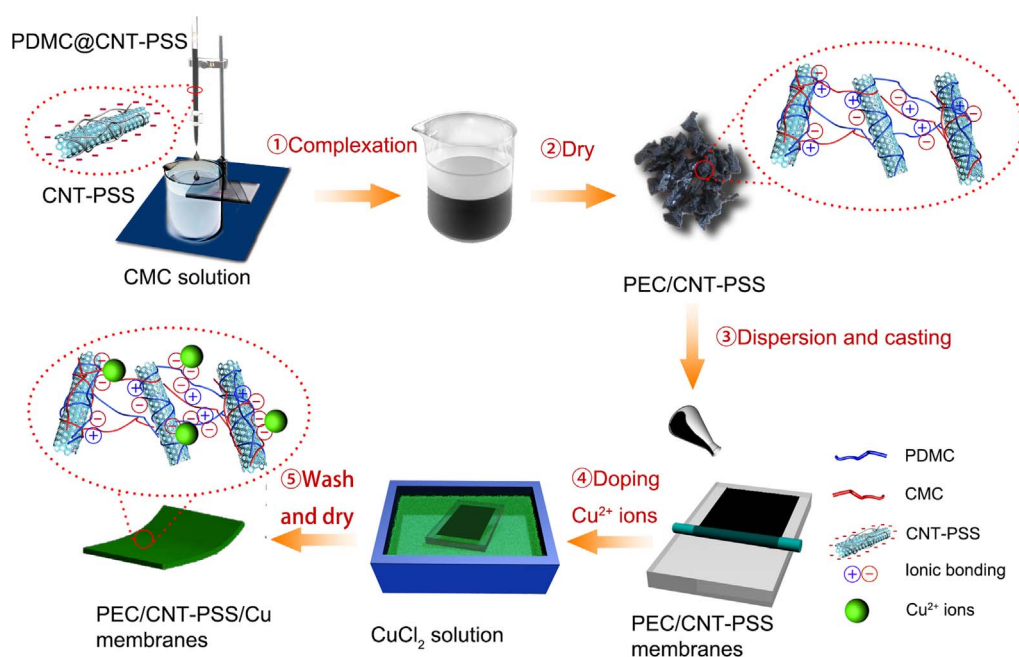


Figure 1 | Schematic diagram for the preparation of PEC/CNT-PSS/Cu membranes.

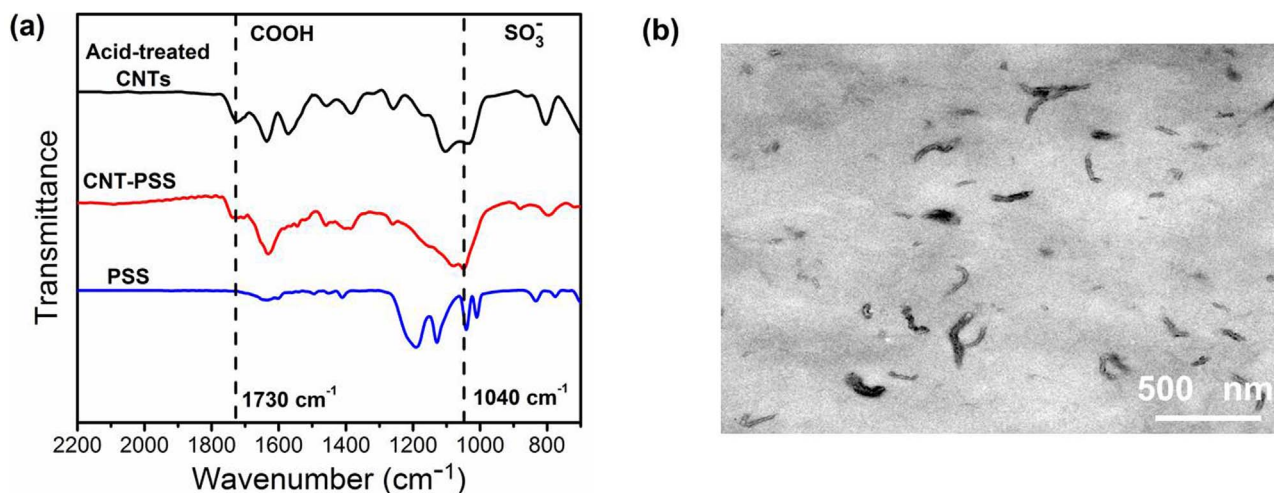


Figure 2 | (a) FTIR spectra of acid-treated CNTs, CNT-PSS, and PSS, (b) a representative TEM image of a PEC/CNT-PSS membrane with 1 wt% CNT-PSS.

improved by factors 2.5 and 2.0 times compared with the pristine PEC membranes, respectively (Fig. 3a). We consider this performance impressive because a high percentage of improvement was achieved using relatively low CNT-PSS content. On the other hand, when using unmodified CNTs, the mechanical improvement obtained with similar PECs is less impressive (tensile strength ca. 60 MPa) even at a much higher loading content (7 wt%)³⁴. As such, the exceptional improvement seen in Fig. 3a understandably arises from the surface modification of CNT-PSS that allows for enhanced interactions between the PEC matrix and CNT-PSS and facilitates a desirable distribution of CNT-PSS in PEC matrix (Fig. 2b). The cross-section image of PEC/CNT-PSS membrane with 1.0 wt% CNT-PSS after tensile testing was characterized by SEM (Fig. 3b). The CNT-PSS are homogeneously dispersed and appear to break after loading stress, which causes the enhancement of tensile strength. In this case, the load transfer from the PEC matrix to CNT-PSS is effectively mediated through the stronger ionic interactions between CNT-PSS and the PEC. In the literature we have generally found that higher CNT content is required to realize such a high percentage of improvement in mechanical strength. In this respect a comprehensive comparison is made (Table S1), showing the current nanohybrid system indeed benefits from the surface modification. Moreover, the nanohybrid membrane appears flexible, as we can see that a large degree of bending does not crack the membrane (inset of Fig. 3a).

Although the mechanical reinforcement achieved by incorporating CNT-PSS is efficient we found that PEC/CNT-PSS membranes are sensitive to RH. As seen from Fig. 4, the mechanical properties of PEC/CNT-PSS membranes drastically decrease from 82 MPa to 27 MPa with increasing RH from 30% to 90%, respectively. This vulnerability of strength to RH is likely due to excessive swelling at high RH, severely limiting their practical applications. To rectify this, we incorporate copper ions that can be chelated by carboxylate groups in the PEC/CNT-PSS membranes. It is expected that the chelating structures will depress the swelling and improve the humidity resistance. The effect of Cu^{2+} content on the mechanical properties of PEC membranes is presented in Fig. S6. The PEC membranes with maximum Cu^{2+} content after saturated doping show optimal mechanical properties. Thus, the following discussion about Cu^{2+} ions illustrates that the membranes have achieved the maximum doping in 24 h. The amount of copper in the membranes is 5.28 wt% as derived from EDX (Fig. S7). Strikingly, the tensile strength of PEC/CNT-PSS/Cu membranes decreases from 64 MPa at 60% RH to 55 MPa at 90% RH, which is much higher than PEC/CNT-PSS membranes at the same RH. Moreover, we compared the effect of doping various multivalent ions including Ca^{2+} , Zn^{2+} , Cu^{2+} , and Fe^{3+} on tensile strength (Fig. S8). The tensile strength of doping copper ions is superior to that of the other ions at 90% RH, which is attributed to the strong binding energy of copper-based chelating

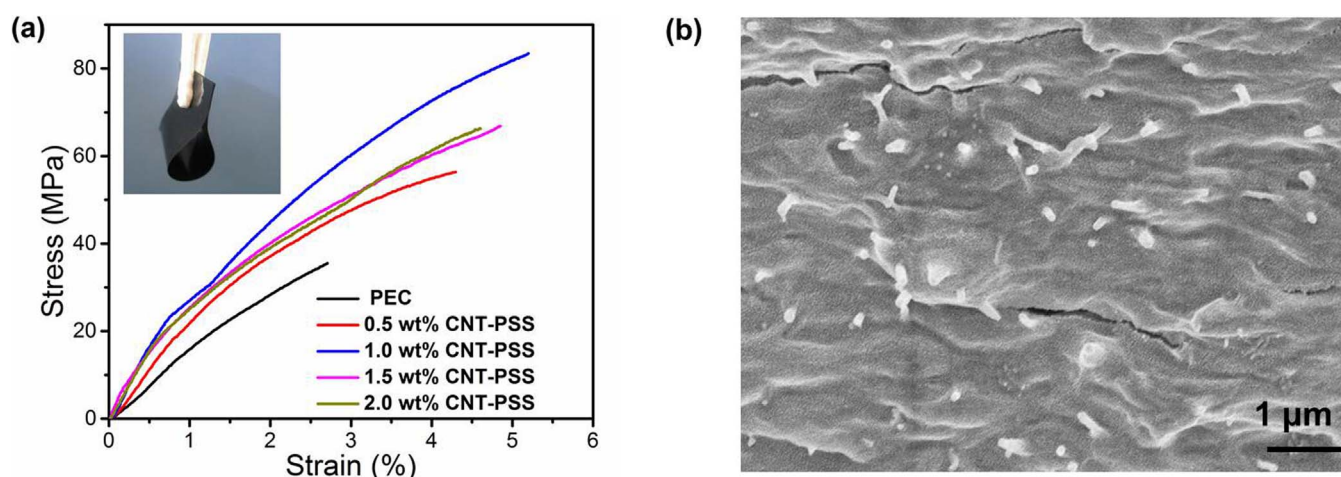


Figure 3 | (a) Stress-strain curves of PEC/CNT-PSS membranes at 30% RH and the insertion is an optical photograph of free-standing PEC/CNT-PSS membrane with 1.0 wt% content, (b) SEM cross-section image of PEC/CNT-PSS membrane with 1.0 wt% content.

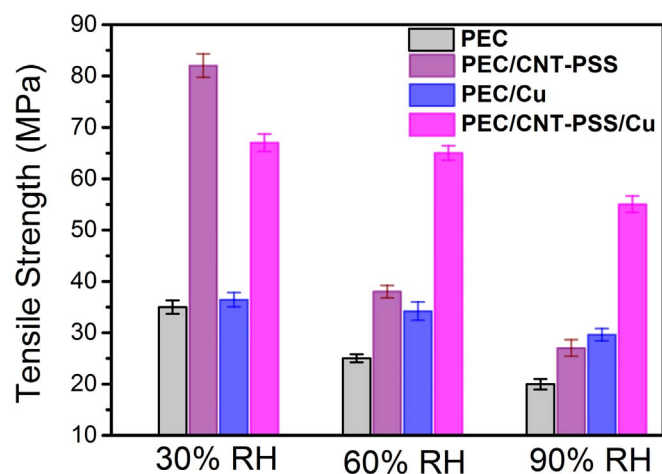


Figure 4 | The tensile strength of membranes at different RH. Please note: the stress-strain curves for obtaining the data of tensile strength are shown in Fig.S9.

structures³⁵. Unfortunately, no distinct or clear trend was found for the effect of these ions^{36,37}. Collectively, Fig. 4 thoroughly demonstrates that neither PEC/Cu nor CNT-PSS membranes possess a high value of tensile strength at high RH. Both of the CNT-PSS and copper ions are required to achieve an excellent tensile strength at high RH.

The mechanism of tensile strength with resistance to the high RH.

Water has a huge effect on the tensile strength of hydrophilic polymers. Usually the decline of tensile strength at high RH (>60%) stems from the absorption of water. Lösche et al. reported that multilayer polyelectrolyte membranes absorbed 40 wt% water at 100% RH³⁸. The tensile strength of double-network hydrophilic polymers decreased dramatically after absorption of large amounts of water (90 wt%)³⁹. The doping of membranes with copper ions reduces plasticizing effect of water by depressing the degree of swelling. The water content in membranes was determined at several different RH (Fig. 5a). In undoped membranes the water content increased from 13 wt% to 43 wt% when the RH was increased from 30% to 90%, respectively. After doping membranes with copper ions, the water content in membranes increased from 7 wt% to 32 wt% over the same RH range. In this scenario, less water was absorbed in membranes with copper ions. Yet, the incorporation of CNT-PSS has no remarkable impact on the water content in membranes.

The chelate structure between copper ions and carboxylic groups (COO^-) was characterized by ATR-FTIR spectroscopy (Fig. 5b). The

marked absorption at 1724 cm^{-1} is assigned to the stretching vibration of carboxylic ester groups ($-\text{COOR}$) from PDMC, while the absorption at 1598 cm^{-1} is ascribed to the stretching vibration of carboxylic groups ($-\text{COO}^-$) from CMC. After doping with copper ions, the peak at 1724 cm^{-1} is retained, but the peak at 1598 cm^{-1} was shifted to 1586 cm^{-1} , with decreased intensity. The red shift is typically interpreted as evidence for the generation of chelate structures after doping copper ions (as shown in the inset of Fig. 5b)⁴⁰. Hence, the reduction of water in membranes may be attributed to the generation of chelate structures.

The schematic model of water in membranes is revealed through a comparison between membranes doped with copper ions and those not doped with copper ions (Fig. 6). On one hand, the loading of CNT-PSS is crucially important for gaining excellent tensile strength, which facilitates the stress transfer and consumes external energy^{41,42}. Outstanding tensile strength at low RH is a prerequisite for achieving high tensile strength at high RH. On the other hand, water absorption in membranes is mainly due to interactions between water and hydrophilic groups, such as hydroxyl groups (OH), carboxylic groups ($-\text{COO}^-$), and others (Fig. S10)⁴³, which produces electrostatic and hydrogen-bonding interactions (Fig. 6a)⁴⁴. After doping with copper ions, the chelate structures formed between copper ions and carboxylic groups, may block the interactions between hydrophilic groups and water thus reducing the water content in membranes (Fig. 6b). The obstruction of interactions is clear when comparing of PEC/CNT-PSS and PEC/CNT-PSS/Cu membranes at 90% RH (Fig. 6). A similar result is acquired using the same method for doping CMC with copper ions (Fig. S11). Moreover, the water contact angle of membranes doped with copper ions increases from $\sim 25^\circ$ to $\sim 45^\circ$, demonstrating that doping with copper ions weakens the interactions between the membrane and water (Fig. S12). Meanwhile, the water contact angle slightly increases after introduction of functionalized carbon nanotubes. In addition, a cross-linked network generated via the chelation is essential for enhanced tensile strength at high RH, whereby water is unable to access to the interior of membranes. The optimal tensile strength is available by the incorporation of both CNT-PSS and copper ions.

Performances of membranes in separating the water/isopropanol mixtures. PECs are good candidates for pervaporation dehydration of alcohols⁴⁵. However, when membranes swell as a result of being subjected to a high water content feed, the real performance is expected to be poor. Accordingly, the mechanical properties of PEC membranes at high water content feed are crucial for practical applications⁴⁶. Mechanical performances of membranes were investigated after their immersion in feeds of 10 wt% and 30 wt% water/isopropanol mixtures (Fig. 7). Increasing the water

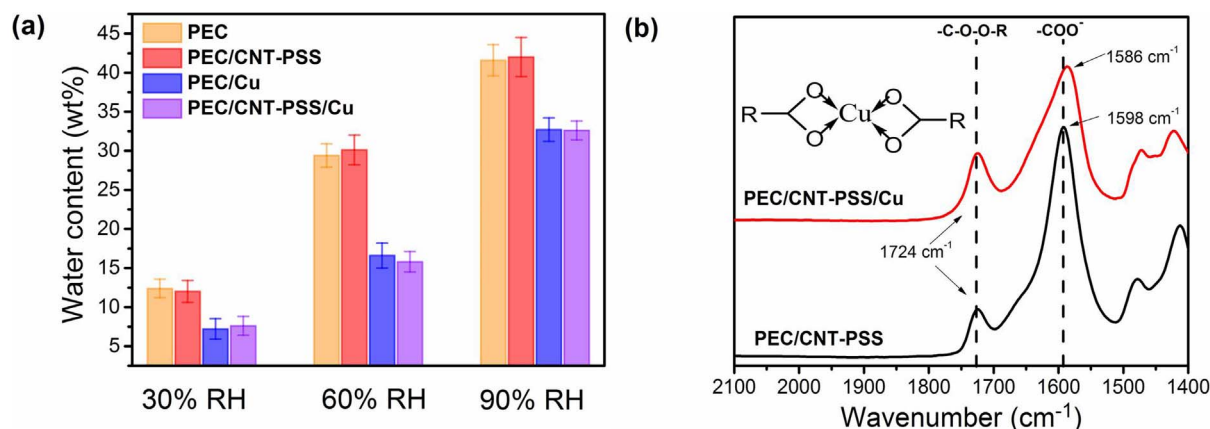


Figure 5 | (a) The water content in membranes at the different RH environment, (b) ATR-FTIR spectra of PEC/CNT-PSS and PEC/CNT-PSS/Cu membranes.

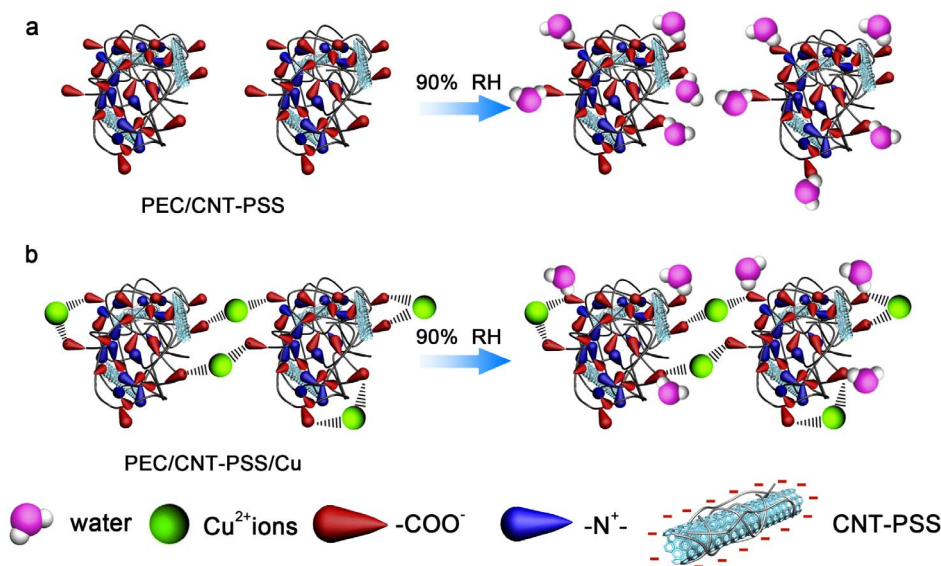


Figure 6 | Schematic model of water absorption in (a) PEC/CNT-PSS membranes and (b) PEC/CNT-PSS/Cu membranes.

content of the feed from 10 wt% to 30 wt% resulted in the tensile strength of PEC, PEC/CNT-PSS and PEC/Cu membranes to decrease from 26 MPa, 32 MPa and 36 MPa to 10 MPa, 16 MPa and 25 MPa, respectively. However, the tensile strength of the PEC/CNT-PSS/Cu membranes decreased from 60 and 43 MPa after the same treatment. This impressive mechanical performance makes them promising alternatives for the dehydration of 30 wt% water/isopropanol mixtures.

Additionally, the pervaporation performances of Cu^{2+} ion doped membranes are demonstrated over the range from 10 wt% to 30 wt% water content at 40°C (Fig. 8). Although the copper ions doped membranes suffer some decline in terms of flux, they are superior to membranes without copper ions in terms of water in permeation. For instance, the water content in permeate of PEC/Cu and PEC/CNT-PSS/Cu membranes was dramatically improved from 90 wt% to 96 wt% in dehydrating 30 wt% water/isopropanol mixtures. The infiltration of copper ions into membranes improves the resistance to the plasticizing effect of water, which means that membranes could endure more water in the feed. This could be connected to the results of Fig. 5a.

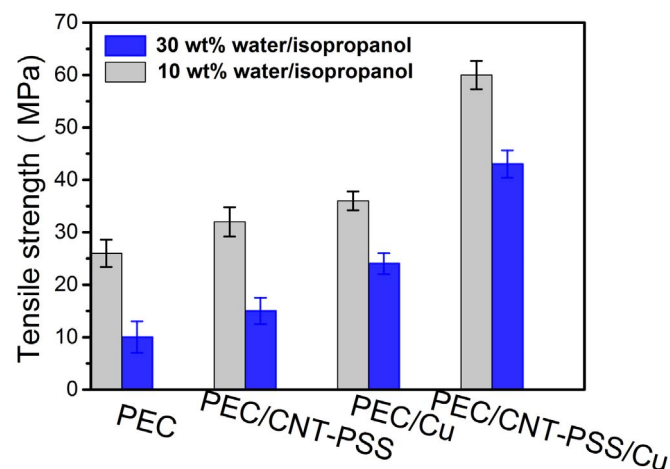


Figure 7 | The tensile strength of membranes doping copper ions after immersing in the feed of 10 wt% and 30 wt% water/isopropanol mixtures.

Conclusions

We have demonstrated a facile method for preparing PEC-based membranes with tensile strengths up to 55 MPa at 90% RH, which is 2.7 times higher than that of pristine PEC membranes under the same conditions. This remarkable enhancement is achieved through the simultaneous incorporation of CNT-PSS (1 wt%) and copper ions (5.28 wt%). The strengthening is attributed to a synergistic effect between the addition of CNT-PSS and copper ions. The CNT-PSS promotes efficient load transfer to increase the mechanical strength, while the copper ions chelate with carboxylic groups and inhibit excessive swelling. After optimization the nanohybrid membranes feature high mechanical strength and good performance in separating aqueous alcohols with water content as high as 30 wt%. For instance, the flux and water content in permeate of PEC/CNT-PSS/Cu membranes is 2200 g/m²h and 96 wt%, respectively. As such, this study illustrates a way to fabricate materials that exhibit good performance in an atmosphere of high relative humidity.

Methods

Materials. Carbon nanotubes (CNTs) (purity >97%) were obtained from Shenzhen Nanotech Port Co., Ltd., China. The CNT diameters were between 10–20 nm, and their lengths were 2 μm on average. Sodium 4-styrenesulfonate monomer and N,N,N,N-tetramethylethylene-diamine were purchased from Aladdin Chemistry Co., Ltd., Shanghai, China. Potassium persulfate was purchased from Xilong Chemical Reagent Factory, Shantou, China and recrystallized from water prior to use. Carboxymethyl cellulose (CMC), with an intrinsic viscosity of 625.1 mL/g in 0.1 M aqueous sodium hydroxide (NaOH) at 30°C, was obtained from Sinapharm Chemical Reagent Co., Ltd., Shanghai, China. Poly (2-methacryloyloxy ethyl trimethylammonium chloride) (PDMA) (Molecular weight = 300,000 g/mol) was purchased from Henyi Chemical Plant, Shanghai, China. All other chemical reagents, including NaOH, hydrochloric acid (HCl), concentrated nitric acid (HNO₃), concentrated sulfuric acid (H₂SO₄), magnesium chloride (MgCl₂), sodium bromide (NaBr), potassium sulfate (K₂SO₄) and copper chloride (CuCl₂) were analytical reagent grade and provided by Sinapharm Chemical Reagent Co., Ltd., Shanghai, China. Deionized water with a resistivity of 18 MΩ·cm was used in all experiments. Poly (vinylidene fluoride) (PVDF) microporous membrane filters (pore size: 0.22 μm) were obtained from Xinya Material Co., Ltd., Shanghai, China. Polysulfone ultrafiltration supporting membranes (molecular weight cut off = 35,000 Da) were provided by the Development Centre of Water Treatment Technology, Hangzhou, China.

Preparation of CNT-PSS. The acid-treated CNTs were prepared by the oxidation of pristine CNTs⁴⁷. 40 mg acid-treated CNTs and 40 mL deionized water were injected into a three-neck flask and then subjected to ultrasonication for 0.5 h. 50 mg sodium 4-styrenesulfonate was added to the flask and stirred for 0.5 h. After three cycles of vacuum treatment and subsequent filling with N₂ using a Schlenk Line, N,N,N,N-tetramethylethylenediamine (10 μL) and potassium persulfate (0.01 g) in H₂O (1 mL) were added to the solution while stirring. Then, free-radical polymerization was allowed to proceed at 35°C for 6 h⁴⁸. The obtained CNT-PSS product was washed

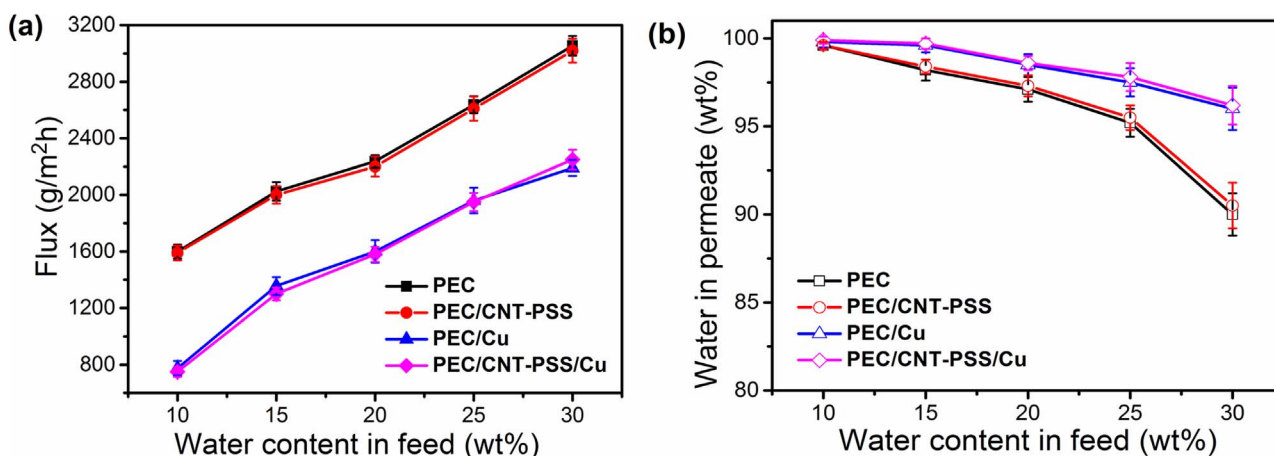


Figure 8 | Pervaporation performances; the flux (a) and water in permeate (b) of membranes in the range of 10 wt% to 30 wt% water/isopropanol mixtures at 40 °C.

with deionized water and then vacuum-filtered through a 0.22 μm PVDF membrane filter. This process was repeated four times to ensure the free PSS in the filtrate was cleared away. The final products were dried overnight under vacuum at 40 °C.

Characterizations. Fourier transform infrared (FTIR) spectra were obtained with an FTIR spectrometer (Bruker Vector 22, Germany). Samples were ground with KBr to prepare pellets and scanned over a range of 400–4000 cm^{-1} . The chemical structures of membranes were characterized with attenuated total reflectance FTIR (ATR-FTIR) (Nicolet 6700, America). Energy dispersive X-ray spectroscopy (EDX) was conducted using an EDX spectrometer (SIRION-100, America). The morphology of the specimen was examined by a scanning electron microscope (SEM, Hitachi S4800, Japan). The specimens were coated with gold prior to SEM examination. Thermogravimetric analysis (TGA) was conducted on a thermal analyzer (PE Pyris 1, America) at a scanning rate of 20 °C/min in nitrogen within the temperature range of 50–800 °C. Transmission electron microscope (TEM) analysis was conducted using a CM200 (Philips, Netherlands) electron microscope at 200 kV. Samples for TEM measurements were prepared by placing 0.1 μL of CNT-PSS onto a copper grid. The mechanical properties of membranes were examined by a universal testing machine (SANS, CTM4204, Shenzhen, China) using a crosshead speed of 2 mm/min. Salts, including MgCl_2 , NaBr and K_2SO_4 , were used to prepare saturated aqueous solutions and create different fixed RH levels. Each sample was allowed to equilibrate at atmospheres of differing RH or with 10 wt% water/isopropanol mixtures for 3 h. Five samples were used for each measurement and their values averaged.

- Nakajima, T. *et al.* A facile method for synthesizing free-shaped and tough double network hydrogels using physically crosslinked poly(vinyl alcohol) as an internal mold. *Polym. Chem.* **1**, 693–697 (2010).
- Zan, X. J., Peng, B., Hoagland, D. A. & Su, Z. H. Polyelectrolyte uptake by PEMs: Impact of salt concentration. *Polym. Chem.* **2**, 2581–2589 (2011).
- Li, G. L. *et al.* Alternating silica/polymer multilayer hybrid microspheres templates for double-shelled polymer and inorganic hollow microstructures. *Chem. Mater.* **22**, 1309–1317 (2010).
- Tang, Z. Y., Kotov, N. A., Magonov, S. & Ozturk, B. Nanostructured artificial nacre. *Nat. Mater.* **2**, 413–418 (2003).
- Yao, H. B. *et al.* 25th anniversary article: Artificial carbonate nanocrystals and layered structural nanocomposites inspired by nacre: Synthesis, fabrication and applications. *Adv. Mater.* **26**, 163–188 (2014).
- Wang, J. F., Cheng, Q. F. & Tang, Z. Y. Layered nanocomposites inspired by the structure and mechanical properties of nacre. *Chem. Soc. Rev.* **41**, 1111–1129 (2012).
- Li, G. L. *et al.* Hybrid nanorattles of metal core and stimuli-responsive polymer shell for confined catalytic reactions. *Polym. Chem.* **2**, 1368–1374 (2011).
- Aindow, T. T. & Neill, J. O. Use of mechanical tests to predict durability of polymer fuel cell membranes under humidity cycling. *J. Power Sources.* **196**, 3851–3854 (2011).
- Verho, T. *et al.* Hydration and dynamic state of nanoconfined polymer layers govern toughness in nacre-mimetic nanocomposites. *Adv. Mater.* **25**, 5055–5059 (2013).
- Müller, C. M. O., Laurindo, J. B. & Yamashita, F. Effect of cellulose fibers on the crystallinity and mechanical properties of starch-based films at different relative humidity values. *Carbohydr. Polym.* **77**, 293–299 (2009).
- Yang, Y., Bolling, L., Haile, M. & Grunlan, J. C. Improving oxygen barrier and reducing moisture sensitivity of weak polyelectrolyte multilayer thin films with crosslinking. *RSC Adv.* **2**, 12355–12363 (2012).
- Das, P. & Walther, A. Ionic supramolecular bonds preserve mechanical properties and enable synergetic performance at high humidity in water-borne, self-assembled nacre-mimetics. *Nanoscale.* **5**, 9348–9356 (2013).

- Lee, S. *et al.* Greatly increased toughness of infiltrated spider silk. *Science.* **324**, 488–492 (2009).
- Thünemann, A. F. *et al.* Polyelectrolyte complexes. *Adv. Polym. Sci.* **166**, 113–171 (2004).
- Gucht, J. V. D., Spruijt, E., Lemmers, M. & Cohen Stuart, M. A. Polyelectrolyte complexes: bulk phases and colloidal systems. *J. Colloid Interf. Sci.* **361**, 407–422 (2011).
- Zhao, Q., Qian, J. W., An, Q. F. & Du, B. Y. Speedy fabrication of free-standing layer-by-layer multilayer films by using polyelectrolyte complex particles as building blocks. *J. Mater. Chem.* **19**, 8448–8455 (2009).
- Joseph, N., Ahmadiannamini, P., Hoogenboom, R. & Vankelecom, I. F. J. Layer-by-layer preparation of polyelectrolyte multilayer membranes for separation. *Polym. Chem.* **5**, 1817–1831 (2014).
- Zhao, Q. *et al.* Hierarchically structured nanoporous poly(ionic liquid) membranes: Facile preparation and application in fiber-optic pH sensing. *J. Am. Chem. Soc.* **135**, 5549–5552 (2013).
- Zhao, Q., Zhang, P. F., Antonietti, M. & Yuan, J. Y. Poly(ionic liquid) complex with spontaneous micro-/mesoporosity: template-free synthesis and application as catalyst support. *J. Am. Chem. Soc.* **134**, 11852–11855 (2012).
- Smitha, B., Sridhar, S. & Khan, A. A. Polyelectrolyte complexes of chitosan and poly(acrylic acid) as proton exchange membranes for fuel cells. *Macromolecules.* **37**, 2233–2239 (2004).
- Zhao, Q. *et al.* An instant multi-responsive porous polymer actuator driven by solvent molecule sorption. *Nat. Commun.* **5**, 4293 (2014).
- Hariri, H. H., Lehaf, A. M. & Schlenoff, J. B. Mechanical properties of osmotically stressed polyelectrolyte complexes and multilayers: Water as a plasticizer. *Macromolecules.* **45**, 9364–9372 (2012).
- Nolte, A. J., Treat, N. D., Cohen, R. E. & Rubner, M. F. Effect of relative humidity on the Young's modulus of polyelectrolyte multilayer films and related nonionic polymers. *Macromolecules.* **41**, 5793–5798 (2008).
- Kusoglu, A. *et al.* Mechanical behavior of fuel cell membranes under humidity cycles and effect of swelling anisotropy on the fatigue stresses. *J. Power Sources.* **170**, 345–358 (2007).
- Huang, X., Schubert, A. B., Chrisman, J. D. & Zacharia, N. S. Formation and tunable disassembly of polyelectrolyte-Cu²⁺ Layer-by-Layer complex film. *Langmuir.* **29**, 12959–12968 (2013).
- Schuetz, P. & Caruso, F. Copper-assisted weak polyelectrolyte multilayer formation on microspheres and subsequent film crosslinking. *Adv. Funct. Mater.* **13**, 929–937 (2003).
- Mentbayeva, A. *et al.* Polymer-metal complexes in polyelectrolyte multilayer films as catalysts for oxidation of toluene. *Langmuir.* **28**, 11948–11955 (2012).
- Krass, H., Papastavrou, G. & Kurth, D. G. Layer-by-Layer self-assembly of a polyelectrolyte bearing metal ion coordination and electrostatic functionality. *Chem. Mater.* **15**, 196–203 (2002).
- Zhao, Q. *et al.* Polyelectrolyte complex membranes for pervaporation, nanofiltration and fuel cell applications. *J. Membr. Sci.* **379**, 19–45 (2011).
- Liu, T. *et al.* Preparation and properties of PEC nanocomposite membranes with carboxymethyl cellulose and modified silica. *Carbohydr. Polym.* **106**, 403–409 (2014).
- Zhao, Q. *et al.* Bio-inspired polyelectrolyte complex/graphene oxide nanocomposite membranes with enhanced tensile strength and ultra-low gas permeability. *Polym. Chem.* **4**, 4298–4302 (2013).
- You, Y. Z., Hong, C. Y. & Pan, C. Y. Directly growing ionic polymers on multi-walled carbon nanotubes via surface RAFT polymerization. *Nanotechnology.* **17**, 2350–2354 (2006).
- Liu, Y. L., Chen, W. H. & Chang, Y. H. Preparation and properties of chitosan/carbon nanotube nanocomposites using poly(styrene sulfonic acid)-modified CNTs. *Carbohydr. Polym.* **76**, 232–238 (2009).



34. Zhao, Q., Qian, J. W., Zhu, M. H. & An, Q. F. Facile fabrication of polyelectrolyte complex/carbon nanotube nanocomposites with improved mechanical properties and ultra-high separation performance. *J. Mater. Chem.* **19**, 8732–8740 (2009).
35. Tomida, T. *et al.* Binding properties of a water-soluble chelating polymer with divalent metal ions measured by ultrafiltration poly(acrylic acid). *Ind. Eng. Chem. Res.* **40**, 3557–3562 (2001).
36. Francolini, I. *et al.* Polyurethane anionomers containing metal ions with antimicrobial properties: Thermal, mechanical and biological characterization. *Acta Biomater.* **6**, 3482–3490 (2010).
37. Park, S. *et al.* Graphene oxide papers modified by divalent ions-enhancing mechanical properties via chemical cross-linking. *ACS Nano.* **2**, 572–578 (2008).
38. Lösche, M. *et al.* Detailed structure of molecularly thin polyelectrolyte multilayer films on solid substrates as revealed by neutron reflectometry. *Macromolecules.* **31**, 8893–8906 (1998).
39. Tominaga, T. *et al.* Hydrophilic double-network polymers that sustain high mechanical modulus under 80% humidity. *ACS Macro Lett.* **1**, 432–436 (2012).
40. Kim, S., Lee, K. & Lee, K. Polyelectrolyte complex membranes based on two anionic polysaccharides composed of sodium alginate and carrageenan: The effect of annealing on the separation of methanol/water mixtures. *J. Appl. Polym. Sci.* **102**, 5781–5788 (2006).
41. Park, J. *et al.* Molecular interactions of polyimides with single-walled carbon nanotubes. *Polym. Chem.* **4**, 290–295 (2013).
42. Thakur, V. K. *et al.* Novel polymer nanocomposites from bioinspired green aqueous functionalization of BNNTs. *Polym. Chem.* **3**, 962–969 (2012).
43. Ping, Z. H. *et al.* States of water in different hydrophilic polymers-DSC and FTIR studies. *Polymer.* **42**, 8461–8467 (2001).
44. Hatakeyama, H. & Hatakeyama, T. Interaction between water and hydrophilic polymers. *Thermochim. Acta* **308**, 3–22 (1998).
45. Liu, T. *et al.* Preparation and characterization of polyelectrolyte complex membranes bearing alkyl side chains for the pervaporation dehydration of alcohols. *J. Membr. Sci.* **429**, 181–189 (2013).
46. Hu, C. L. *et al.* Pervaporation performance of chitosan-poly(acrylic acid) polyelectrolyte complex membranes for dehydration of ethylene glycol aqueous solution. *Sep. Purif. Technol.* **55**, 327–334 (2007).
47. Zhao, X. D. *et al.* Water soluble multi-walled carbon nanotubes prepared via nitroxide-mediated radical polymerization. *J. Mater. Chem.* **16**, 4619–4625 (2006).
48. Qi, J. J. *et al.* Poly(N-isopropylacrylamide) on two-dimensional graphene oxide surfaces. *Polym. Chem.* **3**, 621–624 (2012).

Acknowledgments

This research was financially supported by the NNSFC (51173160, 21376206) and the National Basic Research Program of China (2015CB655303).

Author contributions

T.L., Q.F.A. and Q.Z. devised the original concept, designed the experiments and discussed the interpretation of results. T.L. fabricated the functionalized carbon nanotubes and performed the mechanical testing, pervaporation and the rest experiment. T.L., Q.F.A. and Q.Z. wrote the paper. J.K.W., Y.H.S., B.K.Z. and C.J.G. discussed the results and participated in manuscript revision.

Additional information

Supplementary information accompanies this paper at <http://www.nature.com/scientificreports>

Competing financial interests: The authors declare no competing financial interests.

How to cite this article: Liu, T. *et al.* Synergistic strengthening of polyelectrolyte complex membranes by functionalized carbon nanotubes and metal ions. *Sci. Rep.* **5**, 7782; DOI:10.1038/srep07782 (2015).



This work is licensed under a Creative Commons Attribution-NonCommercial-NoDerivs 4.0 International License. The images or other third party material in this article are included in the article's Creative Commons license, unless indicated otherwise in the credit line; if the material is not included under the Creative Commons license, users will need to obtain permission from the license holder in order to reproduce the material. To view a copy of this license, visit <http://creativecommons.org/licenses/by-nc-nd/4.0/>